

Mechanism and Dynamics of Azobenzene Photoisomerization

Thomas Schultz,[‡] Jason Quenneville,[†] Benjamin Levine,[†] Alessandro Toniolo,[†] Todd J. Martinez,[†] Stefan Lochbrunner,[‡] Michael Schmitt,[‡] James P. Shaffer,[‡] Marek Z. Zgierski,[‡] and Albert Stolow^{*‡}

Stearie Institute for Molecular Sciences, National Research Council of Canada, 100 Sussex Drive, Ottawa, Ontario, Canada K1N 0R6, and Department of Chemistry, University of Illinois, Urbana, Illinois 61801

Received November 18, 2002; Revised Manuscript Received May 1, 2003; E-mail: Albert.Stolow@nrc.ca

Azobenzene (AZ) is considered to be a prototype molecular switch. Its photoisomerization is the basis for many functional materials with applications in photonics¹ and data storage,² as a trigger for protein folding,³ and as probes of local environment.⁴ Although the isomerization proceeds without detectable side reactions, the quantum yield (ϕ_{isom}) displays an unusual wavelength dependence, which violates Kasha's rule.⁵ The excited-state relaxation mechanism underlying this wavelength dependence is still disputed.⁶ We have discovered a new and hitherto uncharacterized excited electronic state, which helps to resolve this controversy.

Here we apply femtosecond (fs) time-resolved photoelectron spectroscopy (TRPES),⁷ supported by excited state ab initio molecular dynamics (AIMD),⁸ to AZ photoisomerization. TRPES has been demonstrated to disentangle electronic from vibrational motions in excited states and has been applied to problems such as excited-state proton transfer and molecular electronic relaxation.⁷ Jet-cooled AZ was excited with a 100 fs laser pulse tuned over the 280–350 nm wavelength range. The excited molecules were probed by ionization with a delayed 207 nm, 100 fs laser pulse. The resulting photoelectron spectrum was measured in a time-of-flight magnetic bottle spectrometer.⁹

In Figure 1, we show a TRPES result for 330 nm excitation. The decay of each energy-integrated photoelectron band yields information about the lifetime of the excited-state involved (see Figure 2, top). The time-integrated photoelectron spectrum allows the identification of the ionic states involved in the ionization process (see Figure 2, bottom). Using Koopmans' theorem, this information can help to identify the nature of the corresponding excited states.¹⁰

Two photoelectron bands α and β with distinct lifetimes were discerned in all TRPES spectra recorded in the wavelength range of 280–340 nm. We deconvoluted bands α and β assuming exponential rise and decay for each band. The 330 nm data in Figure 2 (top) shows laser-limited rise and 170 fs lifetime for band α and laser-limited rise and 420 fs lifetime for β . The immediate rise of α and β shows that both bands are due to direct photoexcitation from the ground state and not to subsequent processes in the excited states. The different lifetimes of the bands indicate the existence of separate decay pathways, likely associated with two electronic states. Other examples for such multistate excitations with distinct relaxation pathways can be found in the literature.¹¹

The photoelectron spectra shown in Figure 2 (bottom) yield vertical ionization potentials of 8.6 and 9.6 eV for the bands α and β , respectively.¹² These values are close to the previously reported vertical ionization potentials for the first (D_0) and third or fourth (D_2 , D_3) ionic states¹³ and α and β were assigned accordingly. The electronic character of the ionic states is known and we assigned the ionization correlations based on Koopmans' theorem:

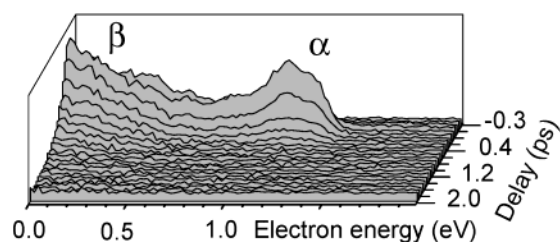


Figure 1. Typical TRPES result, showing the detected electrons as a function of the pump–probe time delay and the photoelectron kinetic energy. Two bands α and β with distinct dynamics were observed.

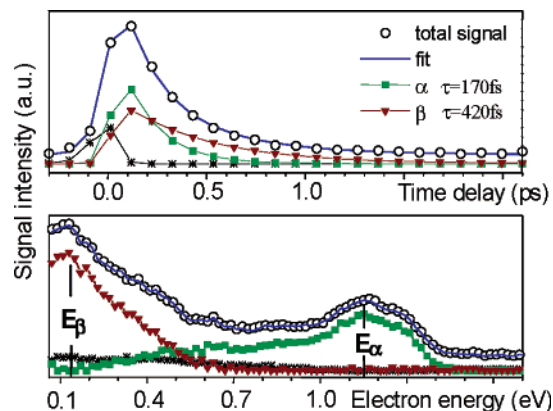


Figure 2. Deconvoluted energy-integrated (top) and time-integrated (bottom) TRPES traces for 330 nm excitation. The fit is the sum of two deconvoluted bands α and β plus a background signal (stars) and fits the total signal at all time delays and electron energies. E_α and E_β denote the positions of the vertical ionization potentials for α and β .

$S_\alpha(\pi_{\text{NN}}\pi^*) \rightarrow D_0(\pi_{\text{NN}}^{-1}) + e^-$, $S_\beta(\pi_\phi\pi^*) \rightarrow D_{2,3}(\pi_\phi^{-1}) + e^-$. As discussed below, we assign α to the ionization of S_2 and β to the ionization of S_3 or S_4 ($S_{3,4}$). The measured decay times of 170 and 420 fs are thus related to the lifetimes of S_2 and $S_{3,4}$.

Multireference ab initio and DFT calculations confirm the existence of three near-degenerate $\pi\pi^*$ states (Table 1).¹⁴ In the lowest state $S_2(\pi_{\text{NN}}\pi^*)$, the excitation is delocalized over the molecule and leads to antibonding character in the N=N double bond. The next two states $S_{3,4}(\pi_\phi\pi^*)$ involve localized excitation in the phenyl rings. One is optically dark by symmetry (1A_g) and can derive intensity only through vibronic coupling.^{15a} The other is optically allowed (1B_u) and has not been previously considered in the S_2 wavelength range. Although the calculated oscillator strengths for S_2 and $S_{3,4}$ given in Table 1 are very sensitive to the geometry (see Supporting Information), the experimental results in Figure 1 indicate that they must be of similar magnitude.

The presence of two absorbing $\pi\pi^*$ states in the energy region hitherto associated with only one can explain the conflicting reports about the reaction coordinates involved in the excited-state relaxation. Three key results in the AZ literature must be explained by

[‡] Steacie Institute for Molecular Sciences, National Research Council of Canada.
[†] University of Illinois.

Table 1. Vertical Excitation Energies E_{Ex} (eV) and Oscillator Strengths f of the Four Lowest Excited States of Azobenzene

character ^a		CASSCF ^b		PT2 ^c	TD-DFT ^d		expt ^e
		E_{ex}	f	E_{ex}	E_{ex}	f	E_{ex}
$S_1(n \rightarrow \pi^*)$	1^1B_g	3.11	0.00	2.34	2.33	0.00	2.79
$S_2(\pi_{\text{NN}} \rightarrow \pi^*)$	1^1B_u	5.56	1.06	4.74	3.78	0.78	3.95
$S_3(\pi_{\phi} \rightarrow \pi^*)$	2^1A_g	5.66	0.00	4.81	4.10	0.00	
$S_4(\pi_{\phi} \rightarrow \pi^*)$	2^1B_u	5.70	0.19	4.76	4.10	0.06	

^a Note the distinct electronic character of the delocalized ($\pi_{\text{NN}} \rightarrow \pi^*$) excitation versus the phenyl ring-localized ($\pi_{\phi} \rightarrow \pi^*$) excitation. ^b State-averaged (five states) complete active space with 10 active electrons in 10 orbitals at SA-1-CAS(10/10)/6-31G optimized minimum with C_{2v} symmetry. ^c Internally contracted CASPT2/6-31G at CAS minimum. ^d $1s$ orbitals of C and N are not correlated. ^e B3LYP/6-31G at the B3LYP/6-31G minimum.

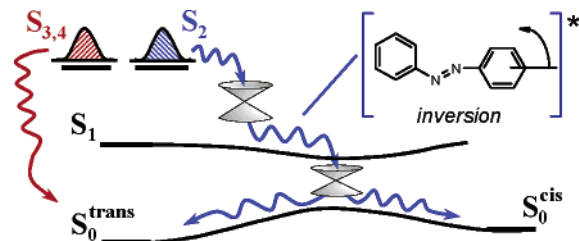


Figure 3. Proposed electronic relaxation pathways for S_2 and $S_{3,4}$: $S_2 \rightarrow S_1$ internal conversion occurs with $\tau = 170$ fs at planar geometry. Subsequent relaxation $S_1 \rightarrow S_0$ is expected to follow Kasha's rule with $\phi_{\text{isom}} \approx 25\%$. The $S_{3,4}$ state with a lifetime $\tau = 430$ fs has a different but not fully characterized relaxation pathway to the trans isomer in S_0 , explaining the reduced $\phi_{\text{isom}} \approx 12\%$ observed for the $\pi\pi^*$ states.

any successful model of the $\pi\pi^*$ state relaxation: (A) the violation of Kasha's rule, i.e., $\phi_{\text{isom}} \approx 25\%$ for $S_1(n\pi^*)$ but $\phi_{\text{isom}} \approx 12\%$ for the higher lying $\pi\pi^*$ state(s);⁵ (B) inhibition of the torsional coordinate in sterically restrained AZ increases ϕ_{isom} of the $\pi\pi^*$ states to a level identical to that observed for S_1 photoexcitation;^{5,16} (C) the observation of efficient relaxation of $S_2(\pi\pi^*)$ to the S_1 state in planar geometry.¹⁷

A relaxation pathway assuming torsional motion in S_2 was suggested by Rau et al. to explain results (A) and (B).⁵ Several time-resolved absorption studies were interpreted with similar models.¹⁸ Theoretical studies supported the existence of a torsional relaxation pathway but disagreed on the states involved in the excited-state relaxation.¹⁵ The torsional relaxation pathway, however, would lead to a twisted conformation in S_1 after internal conversion, in contradiction with result (C).

On the basis of result (C), Fujino et al. presented a different relaxation scheme, assuming the complete absence of a torsional relaxation mode. Result (A) was explained by the presence of an additional unspecified relaxation pathway for high vibrational levels in S_1 . It is difficult, however, to completely reconcile this model with result (B) and with the observation of constant ϕ_{isom} across the S_1 absorption band.⁵

Considering our evidence for a second optically bright state, we developed a new model for the relaxation of the $\pi\pi^*$ states (Figure 3). The $S_2(\pi_{\text{NN}} \rightarrow \pi^*)$ state with a lifetime of 170 fs described here is identical to the short-lived S_2 state (~ 110 fs lifetime) recently observed and internally converts to S_1 in planar geometry (result (C)).¹⁷ We expect the subsequent relaxation of S_1 to follow Kasha's rule and yield $\phi_{\text{isom}} \approx 25\%$ for the population in S_2 . Different relaxation dynamics are observed in the TRPES experiments for $S_{3,4}$, indicating a different relaxation pathway. To explain result (A), we have to assume relaxation of $S_{3,4}$ with reduced isomerization yield. The ring-localized character of $S_{3/4}$ suggests a relaxation

pathway involving phenyl-ring dynamics. This could involve torsion and lead directly to the *trans*-AZ ground state—explaining both results (A) and (B).

AIMD simulations¹⁹ starting from the Franck–Condon geometry in S_2 agree with result (C) and our model and predict that the molecule quickly (< 50 fs) samples geometries near conical intersections while still in a *planar* geometry with no evidence for torsion or inversion. For S_1 , AIMD simulations predict that a conical intersection involving inversion is approached within 50 fs.

In conclusion, we have identified two bright, near-degenerate $\pi\pi^*$ states for AZ with distinct electronic character and decay dynamics. The dissimilar lifetimes of these states suggest different relaxation pathways. The S_2 state involves excitation of the N=N bond and quickly decays to S_1 , retaining planarity. The $S_{3,4}(\pi_{\phi} \rightarrow \pi^*)$ state involves phenyl ring excitation and a different relaxation pathway, leading to a reduced ϕ_{isom} . Our experimentally derived model for the AZ photoisomerization is supported by theory and provides a simple resolution of apparently contradictory results in the literature.

Acknowledgment. We thank T. Tahara for discussions on time-resolved fluorescence experiments. T.S. and J.P.S. thank NSERC Canada for visiting fellowships. S.L. and M.S. thank the German DFG for financial support. Support from NSF (DMR-99-76550 and CHE-02-311876) is acknowledged.

Supporting Information Available: Detailed description and results from ab initio, DFT, and AIMD calculations (PDF). This material is available free of charge via the Internet at <http://pubs.acs.org>.

References

- (1) (a) Ikeda, T.; Sasaki, T.; Ichimura, K. *Nature* **1993**, *361*, 428. (b) Cheben, P.; del Monte, F.; Worsfold, D. J.; Carlsson, D. J.; Grover, C. P.; Mackenzie, J. D. *Nature* **2000**, *408*, 64.
- (2) Åstrand, P.-O.; Ramanujam, P. S.; Hvilsted, S.; Bak, K. L.; Sauer, S. P. A. *J. Am. Chem. Soc.* **2000**, *122*, 3482.
- (3) Spörlein, S.; Carstens, H.; Satzger, H.; Renner, C.; Behrendt, R.; Moroder, L.; Tavan, T.; Zinth, W.; Wachtveitl, J. *Proc. Natl. Acad. Sci. U.S.A.* **2002**, *99*, 7998.
- (4) Kondo, T.; Yoshii, K.; Horie, K.; Itoh, M. *Macromolecules* **2000**, *33*, 3650.
- (5) Rau, H. In *Photochromism: Molecules and Systems*; Dürr, H., Buas-Laurent, H., Eds.; Elsevier: Amsterdam, 1990; pp 165–191.
- (6) Tamai, N.; Miyasaka, H. *Chem. Rev.* **2000**, *100*, 1875.
- (7) (a) Stolow, A. *Annu. Rev. Phys. Chem.* **2003**, *54*, 89. (b) Blanchet, V.; Zgierski, M. Z.; Seideman, T.; Stolow, A. *Nature* **1999**, *401*, 52.
- (8) (a) Martínez, T. J. *Chem. Phys. Lett.* **1996**, *272*, 139. (b) Ben-Nun, M.; Quenneville, J.; Martínez, T. J. *J. Phys. Chem.* **2000**, *104*, 5161.
- (9) Lochbrunner, S.; Larsen, J. J.; Shaffer, J. P.; Schmitt, M.; Schultz, T.; Underwood, J. G.; Stolow, A. *J. Electron. Spectrosc. Relat. Phenom.* **2000**, *112*, 183.
- (10) (a) Blanchet, V.; Zgierski, M. Z.; Stolow, A. *J. Chem. Phys.* **2001**, *114*, 1194. (b) Schmitt, M.; Lochbrunner, S.; Shaffer, J. P.; Larsen, J. J.; Zgierski, M. Z.; Stolow, A. *J. Chem. Phys.* **2001**, *114*, 1206.
- (11) (a) Feng, L.; Huang, X.; Reisler, H. *J. Chem. Phys.* **2002**, *117*, 4820. (b) Hoffman, B. C.; Yarkony, D. R. *J. Chem. Phys.* **2002**, *116*, 8300.
- (12) The ionization potential (IP) is calculated from the measured electron kinetic energy $E_{\alpha,\beta}$ and the photon energies $h\nu_{\text{pump}}$ and $h\nu_{\text{probe}}$ according to $\text{IP} = h\nu_{\text{pump}} + h\nu_{\text{probe}} - E_{\alpha,\beta}$.
- (13) Petrachenko, N. E.; Vovna, V. I.; Furin, G. G. *J. Fluor. Chem.* **1993**, *63*, 85.
- (14) This result is insensitive to dynamic correlation and basis set (see Supporting Information).
- (15) (a) Cattaneo, P.; Persico, M. *Phys. Chem. Chem. Phys.* **1999**, *1*, 4739. (b) Ishikawa, T.; Noro, T.; Shoda, T. *J. Chem. Phys.* **2001**, *115*, 7503.
- (16) Rau, H.; Lüdtke, E. *J. Am. Chem. Soc.* **1982**, *104*, 1616.
- (17) (a) Fujino, T.; Tahara, T. *J. Phys. Chem. A* **2000**, *104*, 4203. (b) Fujino, T.; Arzhantsev, S. Y.; Tahara, T. *J. Phys. Chem. A* **2001**, *105*, 8123.
- (18) (a) Lednev, I. K.; Ye, T. Q.; Matousek, P.; Towrie, M.; Foggi, P.; Neuwahl, F. V. R.; Umaphathy, S.; Hester, R. E.; Moore, J. N. *Chem. Phys. Lett.* **1998**, *290*, 68. (b) Lednev, I. K.; Ye, T. Q.; Abbott, L. C.; Hester, R. E.; Moore, J. N. *J. Phys. Chem. A* **1998**, *102*, 9161. (c) Nägele, T.; Hoche, R.; Zinth, W.; Wachtveitl, J. *Chem. Phys. Lett.* **1997**, *272*, 489.
- (19) AIMD calculations use SA-6-CAS(10/10) wave function, no symmetry restrictions. For details, see Supporting Information.

JA021363X